

## Mpembalike Abnormal Aging Kinetics of Glasses Derived from $\beta$ Relaxation

Lijian Song,<sup>1</sup> Meng Gao<sup>1</sup>, Wei Xu,<sup>1</sup> Juntao Huo<sup>1,\*</sup> and Jun-Qiang Wang<sup>1,2,†</sup>

<sup>1</sup>Zhejiang Key Laboratory of Magnetic Materials and Applications, Ningbo Institute of Materials Technology and Engineering, Chinese Academy of Sciences, Ningbo 315201, China

<sup>2</sup>Center of Materials Science and Optoelectronics Engineering, University of Chinese Academy of Sciences, Beijing 100049, China

 (Received 10 November 2025; revised 12 January 2026; accepted 9 April 2026; published 19 May 2026)

It has been a long, interesting, and mysterious nonequilibrium phenomenon that hot water may freeze faster than warm water, which is known as Mpemba effect. Studying its physical origin and exploring new Mpembalike effects have attracted broad interests. Here, we report experimental evidence of a novel Mpembalike effect in the aging process of glasses: a glass with an initial higher energy state ages (enthalpy decreases) faster and surpasses the glass with an initial lower energy state. This phenomenon is universally observed in different types of structural glasses, including metallic, polymer, and molecular glasses. The underlying thermodynamic mechanism is also studied using high-precision nanocalorimetry. It is found that preannealing at a higher temperature is critical to triggering the faster aging kinetics of the Mpembalike effect. This is attributed to the activation of a secondary  $\beta$  relaxation peak with a substantially lower kinetic barrier than the primary  $\alpha$  relaxation peak. Thus, besides the  $\alpha$  relaxation, the  $\beta$  relaxation plays a pivotal role in the enthalpy aging process, which is very sensitive to the thermal history. These findings may have broad implications for optimizing the thermal treatment and relaxations of different types of glasses.

DOI: [10.1103/znc5-brc6](https://doi.org/10.1103/znc5-brc6)

In the classical paradigm of near-equilibrium systems, a hot or high-energy object should take longer to cool than a cold or low-energy object. Yet, the counterintuitive phenomenon “hot milk can freeze faster into ice-cream” was recorded in the 1960s, the well-known Mpemba effect [1] that could date back 2300 years to the time of Aristotle [2–5]. Since then, the Mpemba effect has been found in many classical systems [2,3,6–20], even in quantum states [21–35]. For example, Kumar and Bechhoefer confirmed that the motion of a colloidal particle at hot temperatures relaxes faster than at cold temperatures by using optical tweezers [2]. Lu and Raz suggested the universality of the Mpemba effect in complex systems based on the typical Ising model [3,9,10,27]. However, the Mpemba effect has not been reported in structural glasses, which are a typical family of nonequilibrium materials.

The classical Mpemba effect on freezing milk or water involves a first-order phase transition, i.e., the nucleation of crystals. The stochasticity of the nucleation processes makes the freezing process very sensitive to environments and has caused extensive debates over the classical Mpemba effect [36–38]. Recently, Baity-Jesi *et al.* found a crossing or intersection phenomenon in the energy aging process of a spin glass, where the initial higher-energy spin glass

surpasses the initial lower-energy spin glass [3]. This is akin to the classical Mpemba effect in freezing water. The aging process of glassy systems lacks a first-order phase transition, which can rule out the influence of stochastic nucleation and thus make these ideal systems to study the universality of the Mpemba effect. However, the classical phenomenological models, such as the Tool-Naraswamy-Moynihan model [39,40], intuitively show that a glass in an initial higher-energy takes longer time than a glass in an initial lower-energy to reach the same low energy, which is contrary to Mpemba effect. Therefore, it is interesting to study whether the Mpembalike effect exists in glasses and, if so, the underlying physical mechanisms.

In this Letter, the aging kinetics of three typical glasses are studied using a high-precision nanocalorimeter (Mettler-Toledo Flash DSC 1): an Au-based metallic glass (MG) in a nominal composition of Au<sub>49</sub>Cu<sub>26.9</sub>Ag<sub>5.5</sub>Pd<sub>2.3</sub>Si<sub>16.3</sub> (at.%), a polyvinyl chloride (PVC) glass, and a sulfur glass. A two-step annealing protocol that first anneals at a high temperature and then at a lower temperature is compared to a one-step annealing protocol at the lower temperature. The high-temperature preannealed glass is controlled to maintain higher or equal enthalpy compared to the lower-temperature preannealed glass. It is interesting to find that, along with the decreasing of enthalpy, the initial high-enthalpy glass surpasses the initial low-enthalpy glass, with an intersection in the time-dependent enthalpy aging curves.

\*Contact author: [huojuntao@nimte.ac.cn](mailto:huojuntao@nimte.ac.cn)

†Contact author: [jqwang@nimte.ac.cn](mailto:jqwang@nimte.ac.cn)

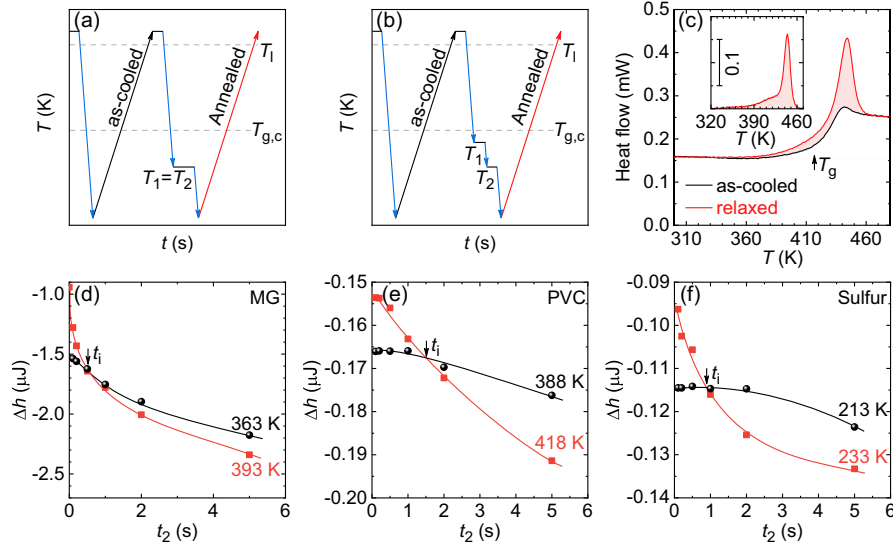


FIG. 1. (a),(b) Schematic illustration of thermal protocols for measuring the DSC trace of as-cooled glass and annealed glass. The cooling rate is  $R_c = 10\,000$  K/s and heating rate is  $R_h = 1\,000$  K/s.  $T_{g,c}$  is the onset glass transition temperature upon cooling. (c) Representative DSC traces of the as-cooled Au-based MG sample and the sample annealed at  $T_1 = 393$  K for  $t_1 = 10$  s and  $T_2 = 363$  K for  $t_2 = 5$  s. Inset is the corresponding relaxation peak obtained by subtracting the two DSC traces. (d) The enthalpy change ( $\Delta h$ ) for MG at  $T_2 = 363$  K, which was preannealed at  $T_1 = 393$  K for  $t_1 = 0.1$  s (red) and  $T_1 = 363$  K for  $t_1 = 1$  s (black), respectively. (e) The  $\Delta h$  for PVC polymer glass at  $T_2 = 388$  K, which was preannealed at  $T_1 = 418$  K for  $t_1 = 20$  s (red) and  $T_1 = 388$  K for  $t_1 = 20$  s (black), respectively. (f) The  $\Delta h$  for sulfur at  $T_2 = 213$  K, which was preannealed at  $T_1 = 233$  K for  $t_1 = 5$  s (red) and  $T_1 = 213$  K for  $t_1 = 10$  s (black), respectively. The two enthalpy curves intersect each other at some time,  $t_i$ , which is a typical characteristic of the Mpemba effect.

This Mpemba-like effect is universally observed in the three glasses with quite different chemical bonds. The underlying physical mechanism is further studied.

The thermal protocols of single annealing and two-step annealing are compared by using Differential scanning calorimetry (DSC) measurements, as shown in Figs. 1(a) and 1(b). Before isothermal annealing, a reference DSC trace of the directly cooled glass is measured, where the cooling rate is  $10\,000$  K/s and the heating rate is  $1\,000$  K/s. For the one-step annealing protocol, the melt is cooled to some temperatures below  $T_{g,c}$  to anneal, and then the annealed glass is heated up to measure the DSC trace at  $1\,000$  K/s, as shown in Fig. 1(a). For the two-step annealing protocol, the sample is first preannealed at a higher temperature  $T_1$  and then annealed at a lower temperature  $T_2$ , as shown in Fig. 1(b). The representative DSC traces of a directly cooled and two-step annealed ( $T_1 = 393$  K for  $t_1 = 10$  s and  $T_2 = 363$  K for  $t_2 = 5$  s) Au-based MG are shown in Fig. 1(c). It is found that the annealed glass has an extra endothermic peak compared to the as-cooled glass around the glass transition temperature  $T_g$ . The relaxation peak is obtained by subtracting the two heat flow traces, as shown in the inset of Fig. 1(c). The enthalpy change  $\Delta h$  is calculated by integrating the heat flow of relaxation peaks,  $\Delta h = \int_{T_a}^{T_1} C_p dT$ , with  $T_a$  representing the lower annealing temperature (usually  $T_2$  is used as  $T_2 \leq T_1$ ),  $T_1$  is the integral upper limit temperature in the

stable supercooled liquid state, and  $C_p$  is specific heat. The PVC glass and sulfur glass both show an endothermic peak after reheating (see Ref. [41]). The time-dependent enthalpy aging process is shown in Figs. 1(d)–1(f). Interestingly, the initial high-enthalpy glass surpasses the initial low-enthalpy glass, with an intersection or crossing at  $t_i$  for the two enthalpy curves. Such an abnormal relaxation behavior is akin to the classic Mpemba effect in freezing water. It is worth noting that this phenomenon is observed in all three glasses with quite different bonding characters, which suggests the effect's universality in glasses.

To study what conditions will trigger the Mpemba-like effect, the influence of the preannealing temperature and the pre-relaxed enthalpy are studied separately. Figures 2(a) and 2(b) show the influence of preannealing temperature. The enthalpy aging process is studied in two protocols, as shown in Fig. 2(a). The first is preannealing the glass isothermally at temperature  $T_1$ , then jumping to a lower temperature  $T_2$  for further aging (two-step aging). The second protocol is annealing only at  $T_2$  (single aging). The enthalpy aging process at  $T_2$  in the two protocols is compared, as shown in Fig. 2(b). In order to make the  $\Delta h$  be the same at different temperatures, the glass is preannealed at  $T_1 = 413$  K for  $t_1 = 0.5$  s (where the glass has a  $\Delta h = 0.175$  kJ/mol when aged to the equilibrium supercooled liquid state; this  $\Delta h$  value is selected as a reference). To reach the same  $\Delta h$ , the glass is preannealed

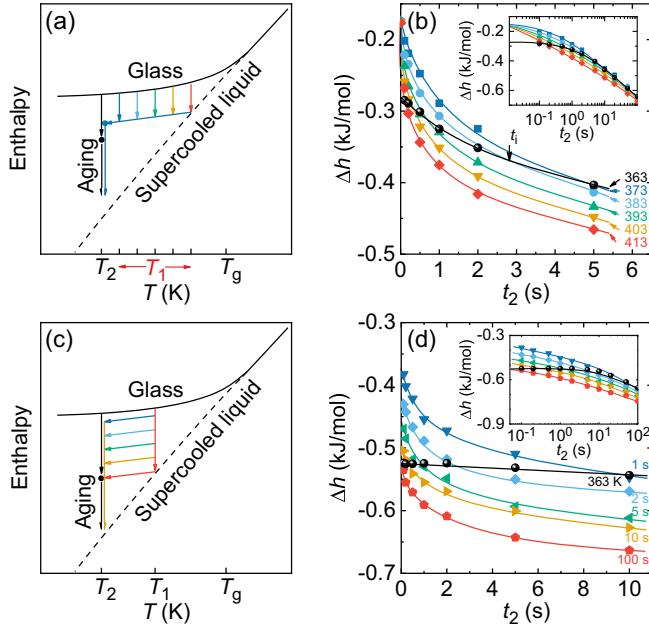


FIG. 2. (a) Isothermal annealing protocol in the space of enthalpy versus temperature for single aging (black) and two-step aging by changing the preannealing temperatures (color). (b) Mpemba effect during enthalpy aging. The enthalpy change ( $\Delta h$ ) at  $T_2 = 363$  K for samples being preannealed at  $T_1 = 363$  K for  $t_1 = 1.0$  s (black),  $T_1 = 373$  K for  $t_1 = 0.17$  s (blue),  $T_1 = 383$  K for  $t_1 = 0.12$  s (cyan),  $T_1 = 393$  K for  $t_1 = 0.1$  s (olive),  $T_1 = 403$  K for  $t_1 = 0.08$  s (orange),  $T_1 = 413$  K for  $t_1 = 0.5$  s (red), respectively. (c) Isothermal annealing protocol in the space of enthalpy versus temperature for single aging (black) and two-step aging by changing the enthalpy states (color). (d) The enthalpy change ( $\Delta h$ ) of the sample at  $T_2 = 363$  K preannealed at  $T_1 = 363$  K for  $t_1 = 20$  s (black) or preannealed at  $T_1 = 393$  K for  $t_1 = 1$  s (blue), 2 s (cyan), 5 s (olive), 10 s (orange), 100 s (red).

at  $T_1 = 403$  K for  $t_1 = 0.08$  s, at  $T_1 = 393$  K for  $t_1 = 0.1$  s, at  $T_1 = 383$  K for  $t_1 = 0.12$  s, and at  $T_1 = 373$  K for  $t_1 = 0.17$  s. All samples were then quenched to  $T_2 = 363$  K. It is found that the enthalpy of samples preannealed at higher temperatures decreased faster than the sample preaged at  $T = 363$  K, with an intersection or crossing at time  $t_i$ . For example, the intersection time  $t_i$  for the glass preannealed at  $T_1 = 383$  K and the reference glass (the sample annealed at 363 K) is about 2.8 s, as shown in Fig. 2(b). A higher preannealing temperature yields a smaller  $t_i$ , suggesting a faster aging rate at low temperature.

The influence of the enthalpy state after preannealing is studied and shown in Figs. 2(c) and 2(d). The schematic thermal protocol in the enthalpy space is shown in Fig. 2(c). The glass is cooled from melt to  $T_1 = 393$  K and isothermally annealed for  $t_1 = 1, 2, 5, 10, 100$  s. Subsequently, the temperature jumps down to a lower  $T_2 = 363$  K at a cooling rate  $R_c = 10000$  K/s and is further annealed isothermally. In Fig. 2(d), the enthalpy

aging process at  $T_2$  is compared with another glass that has been preaged at 363 K for 20 s (whose  $\Delta h$  is almost the same as the glass preannealed at 393 K for 100 s). Interestingly, all the glasses that are preannealed at a higher temperature age much faster, regardless of their initial enthalpy state. These results suggest that the Mpemba effect exists in the enthalpy relaxation process of glass.

To unravel the underlying mechanism of the aging Mpemba effect, the relaxation kinetics is studied. For the glass annealed at a single temperature, 363 K, two representative DSC traces done after annealing at 363 K for 20 s (red trace) and 25 s (blue trace) are shown in Fig. 3(a). The inset shows the subtraction of the two traces, which is composed of a single peak. The height of the relaxation peak increases along with the increase of annealing time, as shown in Fig. 3(b). This confirms the enthalpy aging process. For Debye relaxation, the changing rate of a physical parameter is proportional to itself [44]. Here, the heat flow in DSC measurement corresponds to the energy change rate, which can be given as  $dQ(t)/dt = [Q_0 - Q(t)]/\tau$ . It yields a function to describe the relaxation peak based on the Debye equation [45,46],

$$Q(t) = Q_0 \left[ 1 - \exp\left(-\frac{t}{\tau(T)}\right) \right]. \quad (1)$$

For a continuous heating process, the time  $t$  and temperature  $T$  are related to the heating rate  $R_h$  as  $dT = R_h dt$ . Equation (1) can be reformed into

$$\begin{aligned} Q(t) &= Q_0 \left[ 1 - \exp\left(-\int_{t_s}^t \frac{dt}{\tau(T)}\right) \right] \\ &= Q_0 \left[ 1 - \exp\left(-\int_{T_s}^T \frac{dT}{R_h \tau(T)}\right) \right], \end{aligned} \quad (2)$$

where  $Q_0$  is a constant,  $\tau(T)$  is the temperature-dependent characteristic relaxation time,  $t_s$  is the start time, and  $T_s$  is the start temperature. The  $T$ -dependent relaxation time of  $\beta$  relaxation follows the Arrhenius form  $\tau = \tau_0 \exp(E^*/RT)$ , while the  $T$ -dependent relaxation time of  $\alpha$  relaxation follows the Vogel-Fulcher-Tammann form  $\tau = \tau_0 \exp[DT_0/(T - T_0)]$ . Equation (2) is evaluated numerically, and the continuous heating is replaced by the superposition of a series of isothermal steps,  $\Delta t = \Delta T/R_h$ . The evolution of enthalpy is rewritten as

$$Q(t) = Q_0 \left[ 1 - \exp\left(-\sum_{i=1}^n \frac{\Delta t}{\tau(t_i)}\right) \right]. \quad (3)$$

It suggests that the  $E^*$  of primary  $\alpha$  relaxation peak is about 400 kJ/mol/K [40,47]. The fitting result yields an activation energy of about 488 kJ/mol. This suggests that the aging process is dominated by  $\alpha$  relaxation. It does not change along with annealing time, as shown in Fig. 3(c).

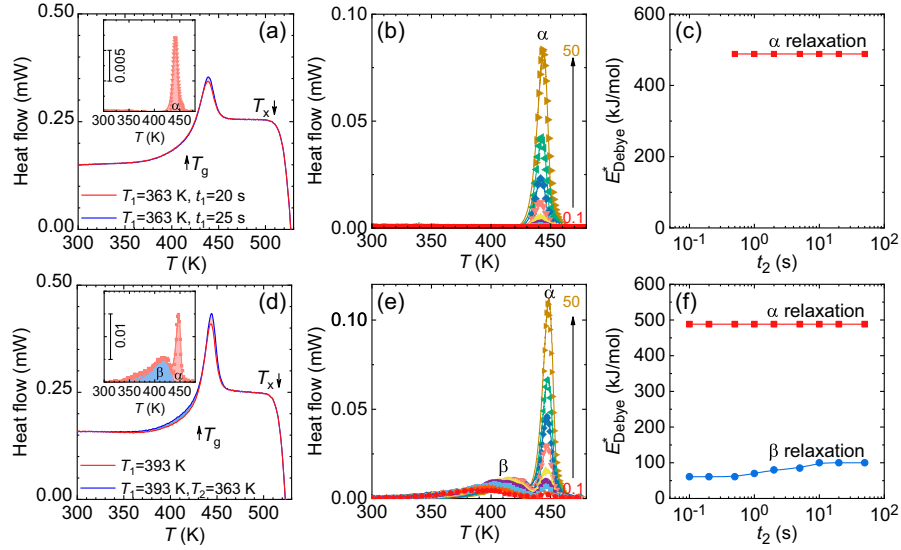


FIG. 3. (a) The heat flow curves measured for heating at a rate of 1000 K/s. Red, the sample annealed at  $T_1 = 363$  K for  $t_1 = 20$  s; blue, the sample annealed at  $T_1 = 363$  K for  $t_1 = 25$  s. Inset is the relaxation trace obtained by subtracting the two traces. (b) The relaxation peak after being annealed at  $T_2 = 363$  K for  $t_2 = 0.1, 0.2, 0.5, 1, 2, 5, 10, 20, 50$  s, respectively. The relaxation peaks are fitted using the Debye model (solid curves). (c) The activation energy of relaxation versus annealing time  $t_2$ . (d) The heat flow curves measured for heating at a rate of 1000 K/s. Red, the sample annealed at  $T_1 = 393$  K for  $t_1 = 10$  s; blue, the sample annealed at  $T_1 = 393$  K for  $t_1 = 10$  s and then annealed at  $T_2 = 363$  K for  $t_2 = 5$  s. Inset is the relaxation trace obtained by subtracting the two traces, which is composed of two peaks. (e) The relaxation peaks after being annealed at  $T_1 = 393$  K for  $t_1 = 10$  s and then annealed at  $T_2 = 363$  K for  $t_2 = 0.1, 0.2, 0.5, 1, 2, 5, 10, 20, 50$  s, respectively. (f) The activation energies of the two relaxation peaks versus annealing time  $t_2$ .

For the two-step aging process, the glass is first annealed at 393 K and further annealed at 363 K. Representative DSC traces are shown in Fig. 3(d). The inset shows the subtraction of the two traces. It is intriguing that the curve is composed of two relaxation peaks. One is around 450 K, and the other is around 400 K. Along with the increase of annealing time, both peaks increase, which indicates a decrease in enthalpy (e.g., aging), as shown in Fig. 3(e). The  $E^*$  of the high-

temperature peak is about 488 kJ/mol, corresponding to the  $\alpha$  relaxation; the  $E^*$  of the low-temperature relaxation peak is about 60–100 kJ/mol/K, which is consistent with the  $26RT_g$  for the  $\beta$  relaxation, as shown in Fig. 3(f). The  $\beta$  relaxation has much smaller activation energy and ages much faster than the  $\alpha$  relaxation.

The contributions of the  $\beta$  relaxation and  $\alpha$  relaxation in the aging process are shown in Fig. 4. For the single

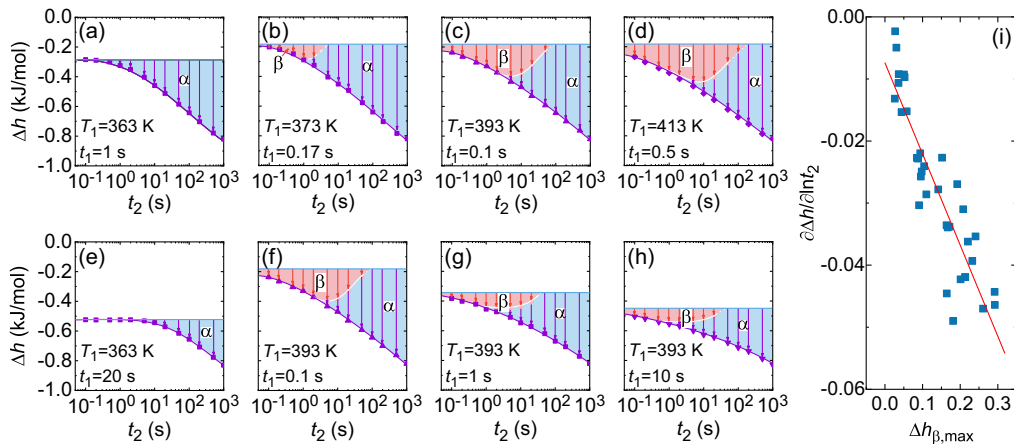


FIG. 4. The time-dependent enthalpy aging process at  $T_2 = 363$  K. (a) The enthalpy change  $\Delta h$  at  $T_2 = 363$  K is caused by  $\alpha$  relaxation (blue shade) when  $T_1 = T_2 = 363$  K,  $t_1 = 1$  s. (b)–(d) The enthalpy change  $\Delta h$  at  $T_2 = 363$  K is caused by both  $\alpha$  relaxation and  $\beta$  relaxation (red shade) when  $T_1 > T_2 = 363$  K. (e) The enthalpy change  $\Delta h$  at  $T_2 = 363$  K is caused by  $\alpha$  relaxation when  $T_1 = T_2 = 363$  K,  $t_1 = 20$  s. (f)–(h) The enthalpy change  $\Delta h$  at  $T_2 = 363$  K is caused by both  $\alpha$  relaxation and  $\beta$  relaxation when  $T_1 > T_2 = 363$  K. (i) The rate of enthalpy change ( $\partial\Delta h/\partial\ln t_2$ ) versus the maximum contribution of  $\beta$  relaxation ( $\Delta h_{\beta,\max}$ ).

relaxation peak [the inset of Fig. 3(a)], the weight of the  $\alpha$  relaxation is the total enthalpy change  $\Delta h$ , while the weights of the  $\alpha$  and  $\beta$  relaxations are calculated based on the proportion of the area of the Debye fitted peaks,  $\Delta h = \Delta h_\beta + \Delta h_\alpha$  [see the inset of Fig. 3(d)]. When  $T_1 = T_2$ , the enthalpy ages only through the  $\alpha$  relaxation and the aging rate is slow, as shown in Figs. 4(a) and 4(e). However, when  $T_1 > T_2 = 363$  K, the enthalpy ages through both the  $\beta$  relaxation and  $\alpha$  relaxation, as shown in Figs. 4(b)–4(d) and 4(f)–4(h). In Figs. 4(b)–4(d), the contribution of the  $\beta$  relaxation increases along with the increase of preannealing temperature. In Figs. 4(f)–4(h), the contribution of the  $\beta$  relaxation decreases along with the increase of preannealing time. The rate of the enthalpy change ( $\partial\Delta h/\partial \ln t_2$ ) exhibits a linear relationship with the amount of  $\beta$  relaxation ( $\Delta h_{\beta, \max}$ , the maximum enthalpy change contributed by the  $\beta$  relaxation), as shown in Fig. 4(i). Thus, the activation of the  $\beta$  relaxation plays a critical role in triggering the Mpemba-like effect.

It is worth comparing the well-known Kovacs memory effect [48,49] in glass with the Mpemba-like effect observed here. These are two typical abnormal relaxation phenomena in glasses. Both effects involve two-step annealing. When the first annealing temperature  $T_1$  is lower than the second annealing temperature  $T_2$ , the Kovacs memory effect would show that the enthalpy *increases* first before further decreasing; when  $T_1 > T_2$ , the Mpemba-like effect shows up. This suggests that the annealing temperatures are noncommutable. The interaction of different relaxation units and the role of entropy in these abnormal phenomena are worth future study.

The classical theories thought that the aging of glasses is conveyed mainly through  $\alpha$  relaxation. However, recent studies have found that there are multiple steps when the glasses relax toward equilibrium [45,50–52]. This Letter demonstrates that the  $\beta$  relaxation plays a pivotal role in glass equilibration, which can accelerate the aging rate during the two-step annealing protocol. Together with previous work [53], it suggests that the  $\beta$  relaxation is sensitive to thermal history. Thus, the space may be quite large for designing the thermal treatment of different types of glasses. Many mysteries are waiting to be explored.

In summary, the Mpemba-like effect is observed in metallic glass, molecular glass, and polymer during the enthalpy aging process. This is a new example of the Mpemba-like effect in disordered materials and suggests the universality of the Mpemba-like effect in glasses. The rapid aging associated with the Mpemba-like effect correlates with the activation of secondary  $\beta$  relaxation. On the other hand, the Mpemba-like effect sheds new light on deepening the understanding of energy control for glasses, as well as optimizing the heat treatment and thermal relaxation of devices.

*Acknowledgments*—We acknowledge financial support from the National Natural Science Foundation of China

(NSFC No. 52525105, No. 52271158, No. U25A20216, and No. U24A2039), National Key R&D Program of China (No. 2024YFB3813702), the Youth Science and Technology Innovation Leading Talent Project of Ningbo (No. 2024QL001), and the Ningbo Major Research and Development Plan Project (No. 2024Z075).

*Data availability*—The data are available from the authors upon reasonable request.

- 
- [1] E. B. Mpemba and D. G. Osborne, Cool?, *Phys. Educ.* **4**, 172 (1969).
  - [2] A. Kumar and J. Bechhoefer, Exponentially faster cooling in a colloidal system, *Nature (London)* **584**, 64 (2020).
  - [3] M. Baity-Jesi, E. Calore, A. Cruz, L. A. Fernandez, J. M. Gil-Narvion, A. Gordillo-Guerrero, D. Iniguez, A. Lasanta, A. Maiorano, E. Marinari *et al.*, The Mpemba effect in spin glasses is a persistent memory effect, *Proc. Natl. Acad. Sci. U.S.A.* **116**, 15350 (2019).
  - [4] M. Jeng, The Mpemba effect: When can hot water freeze faster than cold?, *Am. J. Phys.* **74**, 514 (2006).
  - [5] A. Nava and R. Egger, Pontus-Mpemba effects, *Phys. Rev. Lett.* **135**, 140404 (2025).
  - [6] P. A. Greaney, G. Lani, G. Cicero, and J. C. Grossman, Mpemba-like behavior in carbon nanotube resonators, *Metall. Mater. Trans. A* **42**, 3907 (2011).
  - [7] Y.-H. Ahn, H. Kang, D.-Y. Koh, and H. Lee, Experimental verifications of Mpemba-like behaviors of clathrate hydrates, *Korean J. Chem. Eng.* **33**, 1903 (2016).
  - [8] A. Lasanta, F. Vega Reyes, A. Prados, and A. Santos, When the hotter cools more quickly: Mpemba effect in granular fluids, *Phys. Rev. Lett.* **119**, 148001 (2017).
  - [9] Z. Y. Lu and O. Raz, Nonequilibrium thermodynamics of the Markovian Mpemba effect and its inverse, *Proc. Natl. Acad. Sci. U.S.A.* **114**, 5083 (2017).
  - [10] A. Lapolla and A. Godec, Faster uphill relaxation in thermodynamically equidistant temperature quenches, *Phys. Rev. Lett.* **125**, 110602 (2020).
  - [11] F. J. Schwarzendahl and H. Lowen, Anomalous cooling and overcooling of active colloids, *Phys. Rev. Lett.* **129**, 138002 (2022).
  - [12] A. Kumar, R. Chetrite, and J. Bechhoefer, Anomalous heating in a colloidal system, *Proc. Natl. Acad. Sci. U.S.A.* **119**, e2118484119 (2022).
  - [13] I. Klich, O. Raz, O. Hirschberg, and M. Vucelja, Mpemba index and anomalous relaxation, *Phys. Rev. X* **9**, 021060 (2019).
  - [14] M. Ibáñez, C. Dieball, A. Lasanta, A. Godec, and R. A. Rica, Heating and cooling are fundamentally asymmetric and evolve along distinct pathways, *Nat. Phys.* **20**, 135 (2024).
  - [15] T. Van Vu and H. Hayakawa, Thermomajorization Mpemba effect, *Phys. Rev. Lett.* **134**, 107101 (2025).
  - [16] A. Torrente, M. A. Lopez-Castano, A. Lasanta, F. V. Reyes, A. Prados, and A. Santos, Large Mpemba-like effect in a gas of inelastic rough hard spheres, *Phys. Rev. E* **99**, 060901(R) (2019).

- [17] A. Santos and A. Prados, Mpemba effect in molecular gases under nonlinear drag, *Phys. Fluids* **32**, 072010 (2020).
- [18] A. Megias, A. Santos, and A. Prados, Thermal versus entropic Mpemba effect in molecular gases with nonlinear drag, *Phys. Rev. E* **105**, 054140 (2022).
- [19] T. Van Vu and Y. Hasegawa, Toward relaxation asymmetry: Heating is faster than cooling, *Phys. Rev. Res.* **3**, 043160 (2021).
- [20] A. Biswas, V. V. Prasad, O. Raz, and R. Rajesh, Mpemba effect in driven granular Maxwell gases, *Phys. Rev. E* **102**, 012906 (2020).
- [21] A. K. Chatterjee, S. Takada, and H. Hayakawa, Quantum Mpemba effect in a quantum dot with reservoirs, *Phys. Rev. Lett.* **131**, 080402 (2023).
- [22] L. K. Joshi, J. Franke, A. Rath, F. Ares, S. Murciano, F. Kranzl, R. Blatt, P. Zoller, B. Vermersch, P. Calabrese *et al.*, Observing the quantum Mpemba effect in quantum simulations, *Phys. Rev. Lett.* **133**, 010402 (2024).
- [23] C. Rylands, K. Klobas, F. Ares, P. Calabrese, S. Murciano, and B. Bertini, Microscopic origin of the quantum Mpemba effect in integrable systems, *Phys. Rev. Lett.* **133**, 010401 (2024).
- [24] F. Ares, S. Murciano, and P. Calabrese, Entanglement asymmetry as a probe of symmetry breaking, *Nat. Commun.* **14**, 2036 (2023).
- [25] J. Zhang, G. Xia, C. W. Wu, T. Chen, Q. Zhang, Y. Xie, W. B. Su, W. Wu, C. W. Qiu, P. X. Chen *et al.*, Observation of quantum strong Mpemba effect, *Nat. Commun.* **16**, 301 (2025).
- [26] S. Aharony Shapira, Y. Shapira, J. Markov, G. Teza, N. Akerman, O. Raz, and R. Ozeri, Inverse Mpemba effect demonstrated on a single trapped ion qubit, *Phys. Rev. Lett.* **133**, 010403 (2024).
- [27] F. Carollo, A. Lasanta, and I. Lesanovsky, Exponentially accelerated approach to stationarity in markovian open quantum systems through the Mpemba effect, *Phys. Rev. Lett.* **127**, 060401 (2021).
- [28] A. Nava and R. Egger, Mpemba effects in open non-equilibrium quantum systems, *Phys. Rev. Lett.* **133**, 136302 (2024).
- [29] M. Moroder, O. Culhane, K. Zawadzki, and J. Goold, Thermodynamics of the quantum Mpemba effect, *Phys. Rev. Lett.* **133**, 140404 (2024).
- [30] X. H. Wang and J. Wang, Mpemba effects in nonequilibrium open quantum systems, *Phys. Rev. Res.* **6**, 033330 (2024).
- [31] X. Turkeshi, P. Calabrese, and A. De Luca, Quantum Mpemba effect in random circuits, *Phys. Rev. Lett.* **135**, 040403 (2025).
- [32] D. J. Strachan, A. Purkayastha, and S. R. Clark, Non-Markovian quantum Mpemba effect, *Phys. Rev. Lett.* **134**, 220403 (2025).
- [33] K. Zatsarynna, A. Nava, R. Egger, and A. Zazunov, Green's function approach to Josephson dot dynamics and application to quantum Mpemba effects, *Phys. Rev. B* **111**, 104506 (2025).
- [34] S. Liu, H.-K. Zhang, S. Yin, and S.-X. Zhang, Symmetry restoration and quantum Mpemba effect in symmetric random circuits, *Phys. Rev. Lett.* **133**, 140405 (2024).
- [35] A. Gal and O. Raz, Precooling strategy allows exponentially faster heating, *Phys. Rev. Lett.* **124**, 060602 (2020).
- [36] W. B. Zimmerman, In search of a Mpemba effect protocol: Some hot water does cool and freeze faster than cold, *Chem. Eng. Sci.* **247**, 117043 (2022).
- [37] M. Vynnycky and N. Maeno, Axisymmetric natural convection-driven evaporation of hot water and the Mpemba effect, *Int. J. Heat Mass Transfer* **55**, 7297 (2012).
- [38] J. D. Brownridge, When does hot water freeze faster than cold water? A search for the Mpemba effect, *Am. J. Phys.* **79**, 78 (2011).
- [39] A. Q. Tool, Relaxation between inelastic deformability and thermal expansion of glass in its annealing range, *J. Am. Ceram. Soc.* **29**, 240 (1946).
- [40] O. S. Narayanaswamy, A model of structural relaxation in glass, *J. Am. Ceram. Soc.* **54**, 491 (1971).
- [41] See Supplemental Material at <http://link.aps.org/supplemental/10.1103/znc5-brc6> for the details of experiments, which includes Refs. [42,43].
- [42] R. Zorn, M. Monkenbusch, D. Richter, A. Alegria, J. Colmenero, and B. Farago, Plasticizer effect on the dynamics of polyvinylchloride studied by dielectric spectroscopy and quasielastic neutron scattering, *J. Chem. Phys.* **125**, 154904 (2006).
- [43] P. Yu, W. H. Wang, R. J. Wang, S. X. Lin, X. R. Liu, S. M. Hong, and H. Y. Bai, Understanding exceptional thermodynamic and kinetic stability of amorphous sulfur obtained by rapid compression, *Appl. Phys. Lett.* **94**, 011910 (2009).
- [44] R. M. Hill and L. A. Dissado, Debye and non-Debye relaxation, *J. Phys. C* **18**, 3829 (1985).
- [45] L. J. Song, Y. R. Gao, P. Zou, W. Xu, M. Gao, Y. Zhang, J. T. Huo, F. S. Li, J. C. Qiao, L.-M. Wang *et al.*, Detecting the exponential relaxation spectrum in glasses by high-precision nanocalorimetry, *Proc. Natl. Acad. Sci. U.S.A.* **120**, e2302776120 (2023).
- [46] P. Q. Mantus, Dielectric response of materials extension to the Debye model, *J. Eur. Ceram. Soc.* **19**, 2079 (1999).
- [47] J. Schroers, On the formability of bulk metallic glass in its supercooled liquid state, *Acta Mater.* **56**, 471 (2008).
- [48] L. J. Song, W. Xu, J. T. Huo, F. S. Li, L.-M. Wang, M. D. Ediger, and J.-Q. Wang, Activation entropy as a key factor controlling the memory effect in glasses, *Phys. Rev. Lett.* **125**, 135501 (2020).
- [49] N. C. Keim, J. D. Paulsen, Z. Zeravcic, S. Sastry, and S. R. Nagel, Memory formation in matter, *Rev. Mod. Phys.* **91**, 035002 (2019).
- [50] P. Luo, P. Wen, H. Y. Bai, B. Ruta, and W. H. Wang, Relaxation decoupling in metallic glasses at low temperatures, *Phys. Rev. Lett.* **118**, 225901 (2017).
- [51] I. Gallino, D. Cangialosi, Z. Evenson, L. Schmitt, S. Hechler, M. Stolpe, and B. Ruta, Hierarchical aging pathways and reversible fragile-to-strong transition upon annealing of a metallic glass former, *Acta Mater.* **144**, 400 (2018).
- [52] L. J. Song, W. Xu, J. T. Huo, J.-Q. Wang, X. M. Wang, and R. W. Li, Two-step relaxations in metallic glasses during isothermal annealing, *Intermetallics* **93**, 101 (2018).
- [53] J. N. Wang, L. J. Song, Y. R. Gao, B. W. Zang, M. Gao, J. T. Huo, L. N. Hu, and J.-Q. Wang, Achieving identical glassy state through different thermal paths, *Sci. China Mater.* **66**, 3706 (2023).